Inverse gas chromatography in the characterization of polymeric materials

Agustín Etxeberría, Jokin Alfageme, Cristina Uriarte and Juan J. Iruin*

Departamento de Ciencia y Tecnología de Polímeros, Universidad del País Vasco, Apartado de Correos 1072, San Sebastián (Spain)

ABSTRACT

Different experimental results are presented for the use of inverse gas chromatography in the determination of the physico-chemical properties of pure polymers, polymer solutions and polymer blends. Using poly(hydroxy ether of bisphenol-A) (Phenoxy), its solutions and its blends with other polymers, thermal transitions, polymer solubility parameters, polymer–solvent and polymer–polymer interaction parameters and diffusion coefficients of small molecules in pure Phenoxy have been measured by inverse gas chromatography.

INTRODUCTION

Gas chromatography (GC) is based on the distribution of a compound between two phases. In gas–solid chromatography (GSC) the phases are gas and solid. The injected compound is carried by the gas through a column filled with solid phase, and partitioning occurs via the sorption–desorption of the compound (probe) as it travels past the solid. Separation of two or more components injected simultaneously occurs as a result of differing affinities for the stationary phase. In gas–liquid chromatography (GLC), the stationary phase is a liquid coated on a solid support.

In inverse GC [1], the species of interest is the stationary phase, which usually consist of a polymer-coated support of finely ground polymer mixed with an inert support. This is in contrast to conventional analytical GC, where the stationary phase is of interest only as far as its ability to separate the injected compounds is concerned. Also, in inverse GC, usually only one pure compound (standard solvent or probe) at a time is injected.

The knowledge of the retention volume due to the dissolution of a substance makes it possible to calculate relevant thermodynamic characteristics of the solution process, namely the partition coefficient, the activity coefficient and the change in the excess partial molar thermodynamic functions of the solute in the given stationary phase [2–7].

This technique has also been used in determining other polymer properties such as glass transition temperatures, as reported by Smidrød and Guillet [8,9], melting temperatures [10] and the degree of crystallinity of the polymer [11,12]. On the other hand, GLC has received general recognition as an effective and simple technique for the rapid measurement of polymer-solubility parameters [13,14] (by applying the Hildebrand–Scatchard theory) and polymer–solvent interactions in molten homopolymers [15,16]. Further, Galin and Maslinko [17] have showed that inverse GC can be used for studying polymer–solvent pairs which can be considered as model compounds of polymer–polymer systems. From this type of measurement, predictions about polymer–polymer miscibility can be made.

The study of the interactions between a homopolymer and a volatile probe by means of inverse GC was extended to the investigation of polymer blends. The miscibility of blends such as poly(vinyl chloride) (PVC)–polycaprolactone (PCL) [18], polystyrene (PS)–poly(vinyl methyl ether) (PVME) [19–21], PS–polydimethylsiloxane (PDMS) [22], PS–poly(butyl methacrylate) (PBMA) [23] and poly(methyl acrylate) (PMA)–poly(epichlorohydrin) (PECH) [24] has been studied by analysing the

interaction between the volatile probe (1) and each of the two non-volatile components (2 and 3), and then with a mixture of components 2 and 3. In general, the classical Flory–Huggins theory [25] can be used to interpret the results and to determine the polymer–polymer interaction parameter χ'_{23}, which is a measure of the thermodynamic miscibility of the two polymers.

On the other hand, some workers [26] have determined the temperature of the phase separation of mixed systems by observing their corresponding chromatographic retention diagrams.

Finally, the shapes of eluted peaks in GC on polymeric substrates are governed by several factors, one of the most important being the slow diffusion in the polymer phase. By a suitable choice of conditions, the simple Van Deemter equation [27] enables diffusion coefficients to be calculated from the variation of the chromatographic peak width with carrier gas flow-rate [28].

The objective of this paper is to present different experimental results concerning the use of inverse GC in the determination of the above-mentioned physico-chemical magnitudes using poly(hydroxy ether of bisphenol-A) (Phenoxy; PH), poly(vinylmethyl ether) (PVME), poly(ethylene oxide) (PEO) and their blends, PVME–PH and PEO–PH.

EXPERIMENTAL

Apparatus and procedures

The columns were prepared in the usual manner [29]. The pure polymers and the polymer blends were coated from a solvent solution on to the packing support. After drying in a vacuum oven for *ca.* 48 h at 323 K, the coated support was packed into a ¼-in. O.D. stainless-steel column by applying vacuum to the end. Glass-wool was used to block the ends of the columns. The relative concentration of the polymer in the blends was assumed to be identical with that in the original solution prior to the deposition on the inert support. A description of the columns is given in Table I.

Measurements were made on a modified Perkin-Elmer (Norwalk, CT, USA) Sigma 300 gas chromatograph equipped with a flame ionization detector. Nitrogen was used as the carrier gas. Methane was used as a non-interacting marker to correct the dead volume in the column and the retention time was measured directly with the aid of an Olivetti M-24 microcomputer, equipped with a CHROM + card and appropriate software. A minimum of four measurements were taken for every molecular probe and for each temperature in all columns. Pressures at the inlet and outlet of the column, read from a

TABLE I

DESCRIPTION OF THE GAS CHROMATOGRAPHIC COLUMNS

Column No.	Length (m)	Packing support	Mass of packing in column (g)	Polymer coating	Mass of coating in column (g)
1	0.1	80–100-mesh Chromosorb W AW DMCS	4.4071	PVME	0.4415
2	0.1	80–100-mesh Chromosorb W AW DMCS	4.9757	PEO	0.4966
3	0.1	80–100-mesh Chromosorb W AW DMCS	4.9978	Phenoxy resin	0.5028
4	0.1	80–100-mesh Chromosorb W AW DMCS	4.9196	Phenoxy–PVME (60:40)	0.4941
5	0.1	80–100-mesh Chromosorb W AW DMCS	4.9919	Phenoxy–PEO (50:50)	0.4926
6	0.1	60–80-mesh glass beads	34.1981	Phenoxy resin	0.3549

mercury manometer, were used to calculate corrected retention volumes by the usual procedures. Flow-rates were measured at the end of the column with a soap bubble flow meter.

Columns were conditioned at temperatures above the glass transition temperature (T_g) for *ca.* 48 h prior to use, while nitrogen was flushed through the column in order to achieve equilibrium. The oven temperature was measured within ± 0.1 K over the whole temperature range. The molecular probes, including a small amount of methane marker (<0.01 μl in total), were injected manually with a 10-μl Hamilton syringe.

Materials

Phenoxy was obtained from Quimidroga (Barcelona, Spain) and corresponds to the PKHH product of Union Carbide. The commercial sample, after being purified by dissolution in dioxane and precipitation in methanol, had an average molecular mass, measured by gel permeation chromatography (GPC) (Waters 150-C ALC/GPC system, Waters–Millipore, Milford, MA, USA) in tetrahydrofuran (THF) at 303 K of $\bar{M}_n = 18\,000$ ($\bar{M}_w/\bar{M}_n = 2.8$) [30] (where $\bar{M}_n$ is the average number-average molecular mass and $\bar{M}_w$ is the average mass-average molecular mass).

Poly(vinyl methyl ether) (PVME) ($T_g = 245$ K) was obtained from Polysciences (catalogue no. 3032) and purified in a benzene–isooctane mixture. Its molecular mass, measured by GPC in THF at 303 K, was $\bar{M}_n = 29\,000$ ($\bar{M}_w/\bar{M}_n = 2.1$) [31].

Polyethylene oxide (PEO) was obtained from Union Carbide and corresponds to the WSR-35 product. It was purified in a benzene–n-heptane mixture and its molecular mass was $M_v = 365\,000$, measured by viscometry in benzene [32].

All the solutes (probes) were of chromatographic or analytical-reagent grade and were used without further purification.

Computations

Specific retention volumes were calculated using

$$V_g^0 = \Delta t \cdot \frac{F}{w_L} \cdot \frac{273.16}{T_r} \cdot \frac{3}{2} \cdot \frac{(P_i/P_o)^2 - 1}{(P_i/P_o)^3 - 1} \qquad (1)$$

where $\Delta t = t_p - t_m$ is the difference between the retention times of the probe and the marker, F is the flow-rate of the carrier gas at room temperature (T_r),

w_L is the mass of the stationary phase (weight of the coated polymer in the column) and P_i and P_o are the inlet and outlet pressures, respectively.

RESULTS AND DISCUSSION

The graph of the logarithm of retention volume *versus* reciprocal of the temperature (retention diagram) is a straight line when the polymer is in a fixed state (solid, liquid), the slope being related to the solution enthalpy in GLC or to the adsorption process in GSC:

$$\frac{\partial \ln V_g}{\partial (1/T)} = -\frac{\Delta H}{R} \qquad (2)$$

where ΔH is the enthalpy of the process and R is the gas constant. As a result of a phase transition, the original polymeric stationary phase changes into a different state which must have, in general, different physico-chemical properties. This change is reflected in the retention diagram.

Smidrød and Guillet [9] were the first to use the inverse GC technique to investigate the glass transition in a polymeric material [poly-(N-isopropylacrylamide)]. The retention diagram, which would normally give a straight line, gave curves with a minimum, and this was interpreted as being due to a glass transition which was confirmed by using differential scanning calorimetry. Lavie and Guillet [33] extended this study to the glass transitions of other polymers such as poly(methyl methacrylate) (PMMA), PS and PVC.

The shape of the diagram was explained by postulating that at temperatures below T_g, the probe interacts only with the surface because the rate of diffusion of the probe through the polymer is too slow to permit significant bulk interaction. Several degrees above T_g, the retention volume is a measure of the interaction of the probe with the bulk polymer. Close to T_g both factors contribute to retention. As the temperature rises, the increasing penetrability outweights the effects of increasing vapour pressure, so that retention volumes increase with increasing temperature in this region. This is the intermediate region where diffusion of probe molecules into the polymer matrix is too slow to permit complete equilibrium to be reached within the chromatographic time scale.

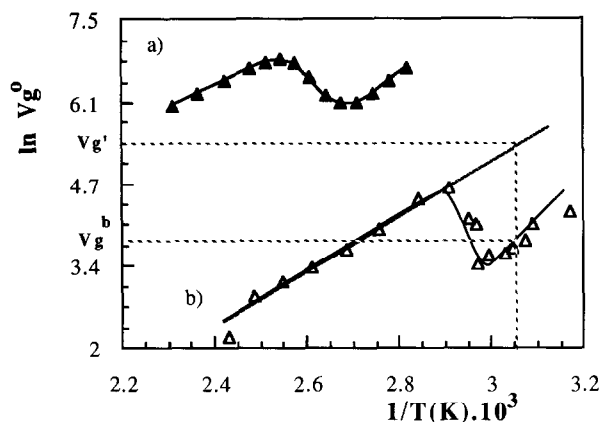The retention diagram of the Phenoxy resin with

Fig. 1. (a) Retention diagram of Phenoxy resin with *n*-decane in the temperature range 353–433 K including the glass transition temperature (T_g). (b) Retention diagram of PEO with benzene in the temperature range 313–413 K including the melting temperature (T_m).

n-decane (Fig. 1a) shows a deviation of the straight line due to the glass transition. When the polymer begin to flow, that is, in the glass transition, the retention volume of the probe increases until a maximum when the whole stationary phase has changed its state. Then, as temperature increases, the probe volatility increases and the retention volume is smaller.

A similar phenomenon occurs in the phase transformation of semicrystalline polymers. Fig. 1b shows the retention diagram of PEO with benzene in a temperature range including the melting temperature (T_m). In this case, below T_m the crystalline regions are impenetrable and the retention volume is due to the amorphous portion of the polymer. Then the polymer melts and one observes the characteristic maximum, after which the whole polymer mass takes part in the dissolution of the sample molecules.

An important contribution to the development of inverse GC for the study of phase transitions in polymeric materials was made by Guillet and co-workers [9,12]. They proposed a method for determining the crystallinity of polymers from retention diagrams.

The determination of crystallinity of polymeric stationary phases is based on the different solubilities of the probe in the crystalline and amorphous regions. In fact, as it is assumed that in the range below T_m the crystalline regions do not participate in

the retention of the molecules of the probe, it is possible to estimate the degree of crystallinity of the sample. Indeed, the extrapolation of the line above T_m into the temperature range below the melting point makes it possible to estimate the retention volume that would correspond to the hypothetical amorphous state of the entire polymer in this temperature range. If we do this on the PEO retention diagram, we can calculate the percentage of crystallinity (PC) by means of the equation

$$PC = 100\left(1 - \frac{V_g^b}{V_g'}\right) \qquad (3)$$

where V_g' and V_g^b are the extrapolated and measured values of the unit retention volume at a given temperature, respectively (see Fig. 1).

Fig. 2 shows the average crystallinity of PEO at different temperatures from data for different probes. A crystalline fraction value of 0.85 for PEO below T_m is in accord with values quoted by Bergman [34] (0.8 and 0.9 for PEO samples of molecular masses 8000 and 300 000, respectively) derived from NMR and X-ray methods.

As is well known, a knowledge of the retention volume due to the dissolution of a substance makes it possible to calculate important thermodynamic characteristics of the solution process, namely the partition coefficient, the activity coefficient and excess partial molar thermodynamic functions of the solute in the given stationary phase.

Partial molar activity coefficients at infinite dilution can be calculated using

$$\ln(a_1/w_1)^\infty = \ln\left(\frac{273.16R}{P_1^0 V_g^0 M_1}\right) - P_1^0(B_{11} - V_1)/RT \qquad (4)$$
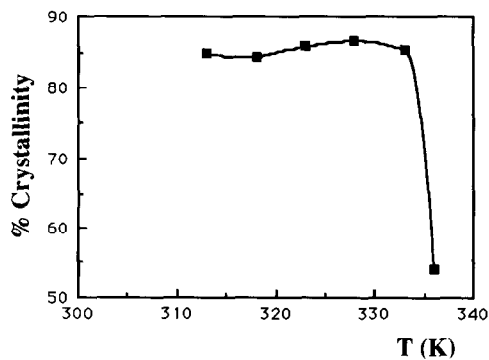

Fig. 2. Evolution of PEO crystallinity with temperature from IGC data.

The application of GC in studying the thermo-dynamics of the interaction of volatile substances with a polymer phase was specially considered by Smidrød and Guillet [9]. They used excess thermo-dynamic functions of mixing at temperatures above the flow-point of the polymer:

$$\overline{\Delta G_1^\infty} = RT \ln (a_1/w_1)^\infty \tag{5}$$

$$\overline{\Delta H_1^\infty} = R \cdot \frac{\partial \ln (a_1/w_1)^\infty}{\partial (1/T)} \tag{6}$$

$$\overline{\Delta S_1^\infty} = \frac{(\overline{\Delta H_1^\infty} - \overline{\Delta G_1^\infty})}{T} \tag{7}$$

where $\overline{\Delta G_1^\infty}$, $\overline{\Delta H_1^\infty}$ and $\overline{\Delta S_1^\infty}$ are the solvent partial molar free energy, enthalpy and entropy of mixing, respectively, at infinite dilution (see Table II).

From the pioneering work of Freeman and Row-linson [35], it has been recognized that polymer solutions can exhibit two critical temperatures, the upper critical solution temperature (UCST) and lower critical solution temperature (LCST). The critical conditions can be elucidated by means of the well known Flory–Huggins interaction parameter, χ, whose physical meaning has been conveniently redefined by modern polymer solution theories. In these new theories, the interaction parameter χ can be understood as an excess partial molar free energy parameter which exhibits a parabolic dependence on

the temperature. The two critical temperatures correspond to the points where χ reaches the $\chi_{crit.}$ value. Between these two points, χ passes through a minimum which gives the maximum of polymer solubility in the solvent.

Inverse GC provides valuable information of the dependence of χ on temperature. Starting with the specific retention volume V_g^0, calculable [25,36] from the retention time of a solvent in a column packed with the polymer, it is possible [25,36] to calculate the interaction parameter χ as

$$\chi = \ln (273.16 R v_{sp,2}/P_1^0 V_g^0 V_1) - 1 -$$
$$[(B_{11} - V_1)/RT]P_1^0 \tag{8}$$

where V_1 is the molar volume of the solvent and $v_{sp,2}$ the specific volume of the polymer.

As we have mentioned before, the inverse GC literature recommends that the inverse GC measurements of thermodynamic properties should be made at a temperature at least 50°C higher than T_g, or a temperature higher than T_m if the polymer is semi-crystalline. This precaution allows us to avoid problems related to slow attainment of the equilibrium in the column, and to render possible the proper comparison of experimental results. In the case of PVME, it exhibits a T_g below room temperature, and therefore retention diagrams were obtained in the temperature range 363–423 K. Linear variations of ln V_g^0 vs. $1/T$ were observed within the temperature range.

Fig. 3 summarizes the χ–T behaviour of different

TABLE II

EXCESS THERMODYNAMIC FUNCTIONS OF MIXING OF THE PHENOXY RESIN WITH VARIOUS PROBES AT 393 K

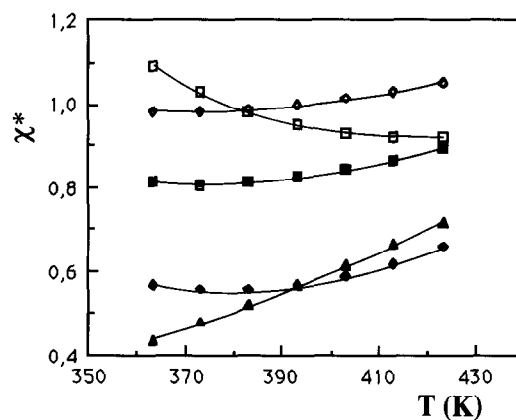| Solvent	$\overline{\Delta G_1^\infty}$ (J/mol)	$\overline{\Delta S_1^\infty}$ (J/mol · K)
Acetonitrile	7 689.76	−18.251
1,2-Dichloroethane	4 998.11	−7.235
Benzene	6 751.87	−3.458
n-Butanone	6 436.84	−11.313
Chlorobenzene	5 479.36	−6.151
n-Decane	12 842.41	16.007
DEGDEE[a]	3 755.11	−25.273
Dioxane	3 973.55	−10.903
Dimethylformamide	2 628.68	−29.891
Ethyl acetate	6 430.77	−18.017
n-Propanol	7 967.40	−13.252
n-Tetradecane	13 531.55	5.393
Toluene	5 479.36	−1.612

[a] DEGDEE = Diethyleneglycol diethyl ether.

Fig. 3. Interaction parameter vs. temperature for the PVME with various probes: ■ = n-decane; ◆ = n-propanol; □ = n-tetradecane; ◇ = acetonitrile; ▲ = n-butanone.

PVME–solvent pairs studied by inverse GC in the range 363–423 K. The curves can be interpreted in all instances as parts of the general parabolic behavior mentioned before. It is important to realize that in inverse GC systems we are in a range of concentrations of $\phi_{\text{solvent}} \to 0$, in precisely the opposite range to that in which the critical conditions are satisfied. However, two important aspects can be inferred from these diagrams.

First, the value of the χ parameter: high values such as those of n-decane correspond to very poor solvents for PVME. In contrast, low values, as for n-butanone, reflect the good solubility capacities of such solvents for the polymer. The second important aspect is the χ–T behavior. Solvents for which χ decreases with increasing T correspond to systems leaving the UCS temperature, as with n-tetradecane in the range 363–423 K. n-Propanol seems to be at the minimum of its parabolic dependence, showing its maximum solubility in this range. Other solvents, such as n-butanone, leave the maximum of solubility towards their LCST.

The high χ values for n-propanol can be explained by the existence of hydrogen bonds in the pure liquid. In the case of acetonitrile its value has been ascribed to the difference in dipolar interactions between pure and diluted acetonitrile.

Of course, this analysis is restriced by the χ value and by the fact that we are in the other extreme of the critical conditions. However, qualitative conclusions similar to those explained above can give a first insight into the quality of different solvents for PVME.

For practical purposes, the so-called solubility parameter has been used as a tool for characterizing polymer solubility in organic liquid, such as those used in coatings. DiPaola-Baranyi and Guillet [13] have shown that inverse GC can be a simple and convenient method for calculating solubility parameters for polymeric stationary phases. The method is based on the fact that the Flory–Huggins χ parameter can be related to solubility parameters by means of a combination of the Hildebrand–Scatchard and Flory theories [25] as follows:

$$\chi = (V_1/RT)(\delta_1 - \delta_2)^2 \qquad (9)$$

where δ_1 is the solubility parameter of the probe and δ_2 is that of the polymer.

TABLE III

SOLUBILITY PARAMETERS OF PHENOXY RESIN AT SEVERAL TEMPERATURES

$\delta_2 \ [(J/m^3)^{1/2} \cdot 10^3]$	T (K)
37.56	373
37.01	383
36.26	393
35.25	403
34.75	413

Following the method developed by DiPaola-Baranyi and Guillet [13], eqn. 9 can be rewritten as

$$(\delta_1^2/RT - \chi/V_1) = (2\delta_2/RT)\delta_1 - \delta_2^2/RT \qquad (10)$$

Therefore, a plot of $(\delta_1^2/RT - \chi/V_1)$ *vs.* δ_1 of the probes will give a straight line with a slope of $2\delta_2/RT$ and an intercept of $-\delta_2^2/RT$. Slopes and intercepts were obtained from a linear least-squares analysis. Derived values of δ_2 for the Phenoxy resin at several temperatures are listed in Table III.

From the extrapolation to 298 K of the data in Table III, we obtain a δ_2 value of $21.10 \cdot 10^{-3}$ $(J/m^3)^{1/2}$. This extrapolatad value is in good agreement with the value derived from a method recently proposed by Coleman *et al.* [37], $\delta_2 = 20.93 \cdot 10^{-3}$ $(J/m^3)^{1/2}$.

Galin and Maslinko [17] showed that inverse GC can be used for predicting polymer–polymer miscibility. They demonstrated that the specific retention volume, V_g^0, and its related magnitude, the partial molar enthalpy of mixing at infinite dilution (ΔH_1^∞), can be used for predicting polymer 1–polymer 2 miscibility [17,30], using systems where the solvent is a model compound for polymer 2.

The average value of ΔH_1^∞ for each solvent can be determined by least-squares analysis of the ln $(a_1/w_1)^\infty$ *vs.* $1/T$ plots. Table IV summarizes experimental ΔH_1^∞ values for the different solvents investigated. It illustrates the capacity of this type of analysis. ΔH_1^∞ becomes negative in solvents such as ethers and esters, reflecting, in a qualitative way, the preference of the Phenoxy resin for this type of interaction. A similar analysis has been carried out by Galin and Maslinko [17] with poly(vinylidene fluoride) (PVDF).

This qualitative analysis can be extended to any

TABLE IV

POLARIZABILITY, P, DIPOLE MOMENT, μ, AND HYDROGEN BOND ACCEPTING POWER, β, OF PURE SOLVENTS AND PARTIAL MOLAR HEATS OF MIXING, ΔH_1^∞, OF THE VARIOUS SOLUTE–PHENOXY SYSTEMS

Solvent	$(\Delta H_1^\infty)_{exp}$ (kJ/mol)	$P \cdot 10^{30}$ (m^3)	μ (D)	β
Chlorobenzene	3.14	12.34	1.71	0.07
Acetonitrile	0.79	4.44	3.94	0
1,2-Dichloroethane	2.22	8.34	1.40	0
n-Propanol	3.52	6.90	3.09	0.95
Benzene	5.48	10.40	0	0.10
n-Decane	19.34	19.1	0	0
Toluene	4.90	12.34	0.37	0.11
Dioxane	−0.54	8.56	0.42	0.37
Dimethylformamide	−9.04	7.85	3.86	0.69
DEGDEE[a]	−6.11	13.8	1.97	0.55
Tetradecane	15.951	26.0	0	0
Ethyl acetate	−1.30	8.83	1.78	0.45
n-Butanone	2.26	8.24	2.70	0.48

[a] See Table II.

Fig. 4. Experimental vs. calculated ΔH_1^∞ values for the various Phenoxy–probe mixtures according to the multiparametric correlation (eqn. 12).

kind of solvent. Experimental values of ΔH_1^∞ can be correlated with probe polarizabilities P, dipole moments μ and Taft's β empirical parameter, which measures the probe hydrogen bond accepting power through the general equation

$$\overline{\Delta H_1^\infty} \text{ (kJ/mol)} = aP + b\mu + d\beta \tag{11}$$

Data for P, μ and β for the different solvents employed are also given in Table IV [17,38–40].

Fig. 4 shows ΔH_1^∞ experimental values compared with calculated values for the different Phenoxy–solvent systems, according to the best fit:

$$\overline{\Delta H_1^\infty} \text{ (kJ/mol)} = 0.145P \text{ (m}^3 \cdot 10^{-30}) -$$
$$0.25 \, \mu \text{ (D)} - 1.63\beta \tag{12}$$

The data summarized in Fig. 4 may be characterized as a random scatter. The correlation coefficient is worse than that obtained by Galin and Maslinko [17] in a similar analysis of PVDF. Whether or not the correlation is correct obviouly depends on the accuracy of the ΔH_1^∞ measurements and on the reliability of the literature data for β. In spite of these shortcomings at the experimental level, this correlation has allowed the PVF$_2$ miscibility with a variety
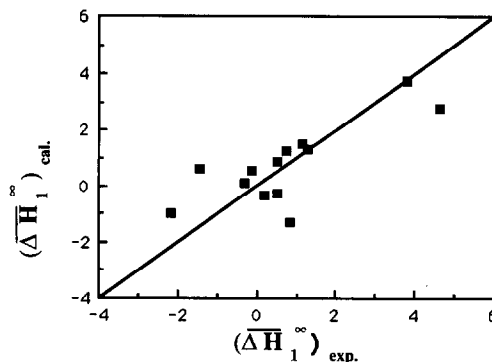
of polyesters to be rationalized and, as may be seen later, it can be used, in a qualitative way, to illustrate the miscibility of Phenoxy with other different polymers. For instance, in the case of N-methylpyrrolidone [model solvent of poly(N-vinylpyrrolidone)], $P = 10.56 \cdot 10^{-30}$ m^3, $\mu = 4.09$ D and $\beta = 0.72$ [31], $(\Delta H_1^\infty)_{cal} = -2.763$ kJ/mol, in good agreement with the well established miscibility of Phenoxy with poly(N-vinylpyrrolidone). In a similar way $(\Delta H_1^\infty)_{cal} = -1.172$ kJ/mol for the system Phenoxy–tetramethylene sulphone. Given the negative values of Phenoxy with ethers and sulphones, the reported miscibility of our resin with a poly(ether sulphone) [40] is not surprising.

The study of the thermodynamics of interaction between a homopolymer and a volatile probe [41] by GLC has been extended to the investigation of ternary systems containing a probe and blends of two polymer components [15].

If the stationary phase is the polymer blend, we can relate the chromatographic data with the interaction parameter between polymers, if the weight fractions of the each homopolymer in the column and the homopolymer–solvent interaction parameter of each component of the blend are known.

Starting with the classical Flory–Huggins expression applied to three-component systems, a method of analysis of inverse GC measurements on polymer blends may be proposed which gives us the polymer–polymer interaction coefficient. In inverse GC, this interaction coefficient is expressed as

$$\chi'_{23} = \frac{\chi_{23}}{x_2} = \frac{\chi_{23}V_1}{V_2} \tag{13}$$

where x_2 is the number of segments in the polymer molecule, V_1 is the molar volume of the solvent injected into the column, V_2 is the molar volume of polymer 2 and χ_{23} and χ'_{23} refer to the interaction between polymer 2 and polymer 3.

Deshpande *et al.* [42] proposed a relationship to obtain such an interaction parameter if we previously know the binary polymer–solvent interaction parameter of each polymer:

$$\left[\left(\frac{\chi_{12}}{V_1} \right) \phi_2 + \left(\frac{\chi_{13}}{V_1} \right) \phi_3 - \left(\frac{\chi_{23}}{V_2} \right) \phi_2 \phi_3 \right] V_1 =$$

$$\ln \left[\frac{273.16 R (w_2 v_{\mathrm{sp},2} + w_3 v_{\mathrm{sp},3})}{P_1^0 V_\mathrm{g}^0 V_1} \right] - \left(1 - \frac{V_1}{V_2} \right) \phi_2 -$$

$$\left(1 - \frac{V_1}{V_3} \right) \phi_3 - \frac{P_1^0}{RT}(B_{11} - V_1) \quad (14)$$

where ϕ_i is the volume fraction of component i and 2 and 3 are the homopolymers.

However, it is easily derivable [24] that the interaction parameter χ'_{23} can be calculated without auxiliary parameters (P_i^0, B_{11}, etc.) by means of

$$\chi'_{23} = \ln \left(\frac{V_{\mathrm{g}_{\mathrm{blend}}}}{w_2 v_{\mathrm{sp},2} + w_3 v_{\mathrm{sp},3}} \right) -$$

$$\left[\phi_2 \ln \left(\frac{V_{\mathrm{g}_2}}{v_{\mathrm{sp},2}} \right) - \phi_3 \ln \left(\frac{V_{\mathrm{g}_3}}{v_{\mathrm{sp},3}} \right) \right] (\phi_2 \phi_3)^{-1} \quad (15)$$

Table V summarizes the binary interaction parameter for several probes and the polymer–polymer interaction parameters for the system PEO–Phenoxy obtained from eqn. 15.

As noted in other chromatographic investigations on polymer–polymer miscibility [31], probe to probe variations are observed. This probe dependence can be explained if we take into account the thermodynamic aspects of a ternary system. χ_{12} and χ_{13} should be obtained in its own ternary system instead of being calculated in the homopolymer–probe binary system. Therefore, the measured χ'_{23} parameter is an apparent parameter which takes into account the real polymer–polymer interaction and other ternary effect not reflected in χ_{12} and χ_{13}.

Galin and Maslinko [43] recently studied the dependence of the PVDF–poly(ethyl methacrylate) (PEMA) interaction parameter on the probe. They observed that a preferential solubility of the probe with respect to one of the components of the blend leads to an artificial increase in the χ'_{23} interaction

TABLE V

POLYMER–SOLVENT BINARY INTERACTION PARAMETERS AND POLYMER–POLYMER INTERACTION PARAMETERS FOR THE SYSTEM PEO–PHENOXY RESIN AND DIFFERENT PROBES OBTAINED FROM EQN. 15 AT 413 K

Solvent	χ_{12}	χ_{13}	χ'_{23}
Toluene	0.652	0.276	0.147
Benzene	0.601	0.124	0.093
Chlorobenzene	0.505	0.045	0.303
1,2-Dichloroethane	0.466	−0.148	0.108
n-Decane	2.101	1.676	0.079
n-Tetradecane	2.435	2.128	0.330
DEGDEE[a]	−0.074	0.086	−0.266
Dioxane	0.015	0.127	−0.289
n-Butanone	0.463	0.391	−0.314
Ethyl acetate	0.579	0.363	−0.272
n-Propanol	0.925	0.458	0.009
Acetonitrile	0.830	0.407	−0.035
Dimethylformamide	−0.335	0.304	−0.176

[a] See Table II.

parameter. Similar results have been obtained for PS–PVME with chlorinated probes [19] and for PVC–PCL with chloroform [18].

The use of a poor solvent of both polymers, such as *n*-decane and *n*-tetradecane, which give high values for χ_{12} and χ_{13}, induces the appearance of diffusion phenomena which yield bad results.

Fig. 5 shows that χ'_{23} interaction parameter at 393 K is an increasing function of $|\Delta\chi| = |\chi_{12} - \chi_{13}|$, but there is no theoretical argument to explain this
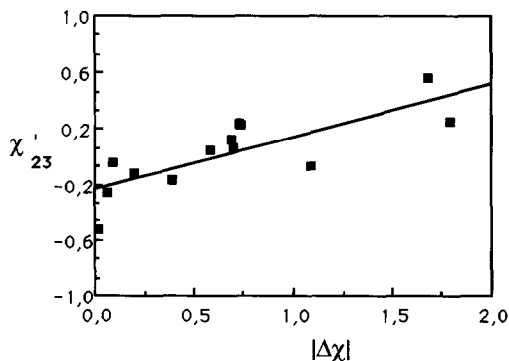

Fig. 5. Variation of χ'_{23} interaction parameter with $|\Delta\chi| = |\chi_{12} - \chi_{13}|$ at 293 K for the PVME–Phenoxy resin system.

dependence. Galin and co-workers [43] observed a similar dependence. Qualitatively, the variation of χ'_{23} with $|\Delta\chi|$ is not surprising. In fact, the preferential interaction of the probe with one of the components of the blend leads to a decrease in $\chi_{1,23}$ in relation with its ideal randomly interaction value. Then there is an artificial increase in χ'_{23}.

Prolongo *et al.* [44] proposed a method for calculating the real polymer–polymer interaction parameter from measurements performed on ternary systems composed of the polymer pairs plus a probe. They obtained an equation, simplified for the IGC data:

$$(\chi_{23})_{app.} = (\chi_{23})_{true} \cdot \frac{s_1}{s_3} +$$
$$+ (\chi_{12} - \chi_{13}) \cdot \frac{(s_3 - s_2) V_2^*}{(\psi_2 s_2 + \psi_3 s_3) V_1^*} \quad (16)$$

where V_i^* is the characteristic molar volume, ψ_i the segment fraction and s_i the number of contact sites per segment of component i.

This equation explains why the interaction parameters determined by IGC are dependent on the probe: they depend on the difference in solvent quality of the probe with regard to the two polymers in the blend, $\chi_{12} - \chi_{13}$, and on the number of contact sites per segment of the solvent s_i.

In order to obtain the $(\chi_{23})_{true}$ value, we rewrite this eqn. 16 as

$$\frac{(\chi_{23})_{app.}}{V_2^* s_1} = \frac{(\chi_{23})_{true}}{V_2^* s_3} +$$
$$+ \frac{(\chi_{12} - \chi_{13})}{V_1^* s_1} \cdot \frac{(s_3 - s_2)}{(\psi_2 s_2 + \psi_3 s_3)} \quad (17)$$

The plot of $(\chi_{23})_{app.}/V_2^* s_1$ versus $\Delta\chi/V_1^* s_1$ should be linear with an intercept $(\chi_{23})_{true}/V_2^* s_3$. Such a type of plot is shown in Fig. 6. The s_1 values needed were calculated according to Bondi [45]. Then the $(\chi_{23})_{true}$ for the PVME–Phenoxy system at 393 K is -0.15.

Phase separation processes can be observed for homopolymer blends using inverse GC. From the chromatographic point of view, the location of the phase separation temperatures can be studied by means of the molecular probe retention volumes in the blend compared with the mean values of the retention volumes of the same molecular probes in the homopolymers. Several workers [23,46–48] have shown that the retention volumes of inmiscible
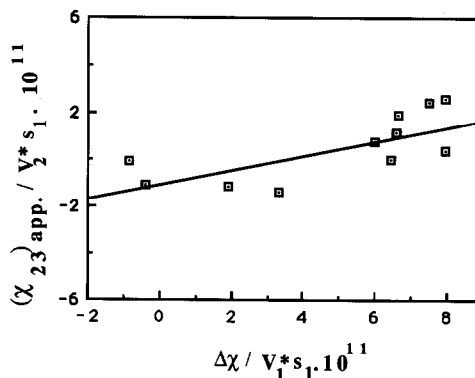

Fig. 6. Representation of $(\chi_{23})_{app.}/V_2^* s_1$ *vs.* $\Delta\chi/V_1^* s_1$ for the PVME–Phenoxy resin system with several probes at 393 K.

blends are a linear combination of the retention volumes of each component:

$$V_g = V_{gl,2} w_2 + V_{gl,3} w_3 \quad (18)$$

Miscible polymer blends have a retention volume lower than the arithmetic average volume of the homopolymers at the corresponding composition because the probe must compete with one of the components for the sites of possible interaction with the other, thus giving a shorter time or volume of elution. In contrast, retention volumes of a phase-separated blend are equal to the linear combination of the retention volumes of the pure constituents.

Retention diagrams of a PVME–Phenoxy blend (40:60) with several molecular probes were determined in the temperature range 384–480 K far from the glass transition temperature of the blend [31]. In all instances, as can be seen in Fig. 7 for *n*-tetra-
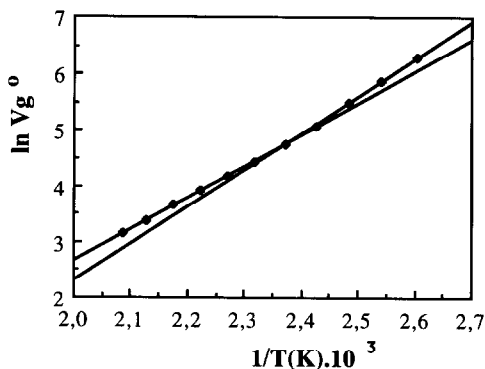

Fig. 7. Retention diagram of PVME–Phenoxy blend (40:60) with *n*-tetradecane in the temperature range 384–480 K including the phase separation temperature.

decane, the diagram showed a deviation from strict linearity between 425 and 445 K. This change in the slope may be identified with the location of the phase separation in the column, and has been confirmed by thermo-optical analysis.

The shapes of eluted peaks in GC on polymeric substrates may have a significant effect on the validity of the data derived from peak retention measurements, and in addition may be related to the thermodynamics and kinetics of the polymer–probe interaction.

One of the most important factors that govern peak shape is slow diffusion in the polymer phase. The method for determining the approximate values of diffusion constants was first reported by Gray and Guillet [28] and utilizes the peak broadening of a probe molecule injected on to a GLC column containing a polymeric stationary phase. Recently, the technique has been extended to coated capillary columns [49].

Van Deemter et al. [27] related peak broadening to column properties through the equation

$$H = A + B/u + Cu \qquad (19)$$

where H is the plate height, u is the linear velocity of the carrier gas and A, B and C are constants independent of u. A and B are related to instrument performance and gas-phase spreading and C is given by

$$C = (8/\pi^2)(d^2/D_1)\left[\frac{k}{(1 + k)^2}\right] \qquad (20)$$

where d is the thickness of the stationary phase, D_1 is the diffusion coefficient of the solute in the stationary phase and k is the partition ratio.

From the resulting plot, the slope C of the linear portion obtained at high velocity ($B/u \to 0$) is determined and D_1 is calculated through eqn. 20, d and k being known.

The average thickness of the stationary phase d was found from the known volume of polymer on the column and the geometric surface area of the beads, which were assumed to be spherical. If this sample bead is coated with a weight w of polymer having a density ρ,

$$d = (w/\rho)/(3 V/r) \qquad (21)$$

where r is an average radius and V is the volume of the sample bead.

The plate height H was determined from the eluted peaks:

$$H = (l/5.54)(w_{1/2}/t_r)^2 \qquad (22)$$

where l is the column length, $w_{1/2}$ is the width of the peak at half-height and t_r is the retention time from the injection to the peak maximum.

The flow-rate was measured at the column outlet in the usual manner. The measured volume flow-rate, F, was converted into linear velocity in the column, u, by the relationship

$$u = (jF/a)(T_c/T_f) \qquad (23)$$

where T_c and T_f are column and flow meter temperatures, a is the volume of gas per unit length of column and j is the James–Martin correction factor of gas compressibility.

The results of a series of experiments to measure the amount of peak spreading as a function of flow-rate for the Phenoxy resin with n-octadecane, a non-polar solvent, are shown in Fig. 8.

At higher flow-rates, H increases linearly with u and C can be determined from the slope. The resulting value of D_1 calculated from the Van Deemter equation is $2.20 \cdot 10^{-6}$ m^2 s^{-1} at 418 K.

The GC measurement of diffusion rates appears to complement the usual sorption and permeation methods, as can be seen in the data obtained by Gray and Guillet [28] for benzene in low-density polyethylene with a resulting value of D_1 of $0.82 \cdot 10^{-4}$ m^2 s^{-1} compared with the value of $1.2 \cdot 10^{-4}$ m^2 s^{-1} obtained by McCall and Slichter [50] using both desorption and time lag measurements.
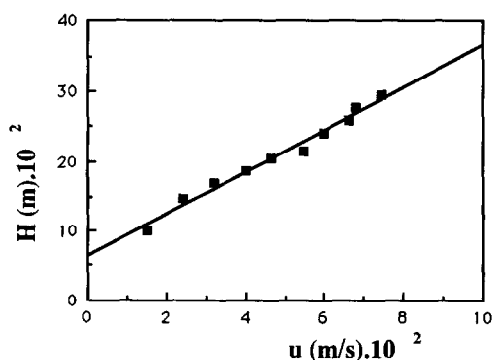

Fig. 8. Representation of the plate height H determined from the Van Deemter equation vs. the linear flow-rate u for a column of Phenoxy on glass beads at 418 K with n-octadecane.

However, use of the simple Van Deemter equation to interpret the GC data may only be valid for relatively non-polar penetrants and polymers at temperatures well above the glass transition temperature of the polymer.

REFERENCES

1 A. V. Kiselev, Adv. Chromatogr., 3(1967) 177.
2 J. M. Braun and J. E. Guillet, Adv. Polym. Sci., 21 (1976) 108.
3 D. G. Gray, Proc. Polym. Sci., 5 (1977) 1.
4 R. J. Laub and R. L. Pecsok, Physicochemical Applications of Gas Chromatography, Wiley, New York, 1978.
5 J. R. Conder and C. L. Young, Physicochemical Measurements by Gas Chromatography, Wiley, New York, 1979.
6 J. E. G. Lipson and J. E. Guillet, in J. V. Dawkins (Editor), Developments in Polymer Characterization, Applied Science Publ., London, 1982, Vol. 3, Ch. 2.
7 G. J. Price, J. E. Guillet and J. H. Purnell, J. Chromatogr., 369 (1986) 273.
8 J. E. Guillet, in J. H. Purnell (Editor), New Developments in Gas Chromatography, Wiley, New York, 1973, p. 187.
9 O. Smidrød and J. E. Guillet, Macromolecules, 2 (1969) 272.
10 G. J. Courval and D. G. Gray, Macromolecules, 8 (1975) 326.
11 J. M. Braun and J. E. Guillet, Macromolecules, 10 (1977) 101.
12 J. E. Guillet and A. N. Stein, Macromolecules, 3 (1979) 102.
13 G. DiPaola-Baranyi and J. E. Guillet, Macromolecules, 11 (1978) 228.
14 K. Ito and J. E. Guillet, Macromolecules, 12 (1979) 1163.
15 D. G. Gray, Prog. Polym. Sci., 5 (1977) 1.
16 J. M. Braun and J. E. Guillet, Adv. Polym. Sci., 21 (1976) 107.
17 M. Galin and L. Maslinko, Macromolecules, 18 (1985) 2192.
18 O. Olabisi, Macromolecules, 8 (1975) 316.
19 C. S. Su and D. Patterson, Macromolecules, 10 (1977) 708.
20 S. Klotz, R. H. Schuster and H.-J. Cantow, Makromol. Chem., 187 (1986) 1491.
21 J. M. Elorza, M. J. Fdz.-Berridi, J. J. Iruin and C. Uriarte, Makromol. Chem., 189 (1988) 1855.
22 M. Galin and M. C. Rupprecht, Macromolecules, 12 (1979) 506.
23 G. DiPaola-Baranyi and P. Degree, Macromolecules, 14 (1981) 1456.
24 Z. Y. Al-Saigh and P. Munk, Macromolecules, 17 (1984) 803.
25 P. J. Flory, Principles of Polymer Chemistry, Cornell University Press, Ithaca, NY, 1953.
26 C. P. Doubé and D. J. Walsh, Eur. Polym. J., 17 (1981) 63.
27 J. J. Van Deemter, F. J. Zuiderweg and A. Klinkenberg, Chem. Eng. Sci., 5 (1966) 271.
28 D. G. Gray and J. E. Guillet, Macromolecules, 6 (1973) 223.
29 M. J. Fernández-Berridi, T. F. Otero, G. M. Guzmán and J. M. Elorza, Polymer, 23 (1982) 1361.
30 J. I. Iribarren, M. Iriarte, C. Uriarte and J. J. Iruin, J. Appl. Polym. Sci., 37 (1989) 3459.
31 C. Uriarte, J. J. Iruin, M. J. Fernández-Berridi and J. M. Elorza, Polymer, 30 (1989) 1155.
32 M. Iriarte, E. Espi, A. Etxeberría, M. Valero, M. J. Fernández-Berridi and J. J. Iruin, Macromolecules, 24 (1991) 5546.
33 A. Lavie and J. E. Guillet, Macromolecules, 2 (1969) 443.
34 K. Bergman, Kolloid-Z. Z. Polym., 251 (1973) 962.
35 P. I. Freeman and J. S. Rowlinson, Polymer, 10 (1960) 2.
36 D. Patterson, Y. B. Tewari, H. P. Schreiber and J. E. Guillet, Macromolecules, 4 (1971) 356.
37 M. M. Coleman, C. J. Serman, D. E. Bhagwagar and P. C. Painter, Polymer, 31 (1990) 1187.
38 K. A. Karim and D. C. Bonner, J. Appl. Polym. Sci., 22 (1978) 1277.
39 M. J. Kamlet, J. L. M. Abboud, M. H. Abraham and R. W. Taft, J. Org. Chem., 48 (1983) 2877.
40 A. L. McClellan, Tables of Experimental Dipole Moments, Rahava Enterprises, El Cerrito, CA, 1974, Vol. 2.
41 V. B. Singh and D. J. Walsh, J. Macromol. Sci. Phys., B25 (1987) 65.
42 D. D. Deshpande, D. Patterson, H. P. Schreiber and C. S. Su, Macromolecules, 7 (1974) 565.
43 M. Galin and L. Maslinko, Eur. Polym. J., 23 (1987) 923.
44 M. G. Prolongo, R. M. Masegosa and A. Horta, Macromolecules, 22 (1989) 4346.
45 A. Bondi, J. Phys. Chem., 64 (1964) 441.
46 C. Zhikuan and D. J. Walsh, Eur. Polym. J., 19 (1983) 519.
47 J. Klein, H. Widdecke and G. Walte, J. Polym. Sci. Polym. Symp., 68 (1980) 221.
48 J. M. Braun and J. E. Guillet, Macromolecules, 9 (1976) 341.
49 D. Arnould and R. L. Laurence, in D. R. Lloyd, H. P. Schreiber and T. C. Ward (Editors), Inverse Gas Chromatography (ACS Symposium Series, No. 391), American Chemical Society, Washington, DC, 1989, Ch. 8, p. 87.
50 D. W. McCall and W. P. Slichter, J. Am. Chem. Soc., 80 (1958) 1861.